Classification: *Biological Sciences-Biochemistry*

Inactivity of Human β,β-Carotene-9',10'-Dioxygenase (BCO2) Underlies Retinal Accumulation of the Human Macular Carotenoid Pigment

Short title: Characterization of Human and Mouse BCO2

Binxing Li[a,1], Preejith P. Vachali[a,1], Aruna Gorusupudi[a], Zhengqing Shen[a], Hassan Sharifzadeh[a], Brian M. Besch[a], Kelly Nelson[a], Madeleine M. Horvath[a], Jeanne M. Frederick[a], Wolfgang Baehr[a,b,c], Paul S. Bernstein[a,2]

[a]Department of Ophthalmology and Visual Sciences, John A. Moran Eye Center, University of Utah School of Medicine, Salt Lake City, UT 84132

[b]Department of Neurobiology and Anatomy, University of Utah School of Medicine, Salt Lake City, UT 84132

[c]Department of Biology, University of Utah, Salt Lake City, UT 84112

[1]Co-first authors

[2] To whom correspondence should be addressed:

Paul S. Bernstein, MD, PhD,

Moran Eye Center, University of Utah
65 Mario Capecchi Drive
Salt Lake City, UT 84132, U. S. A.
Tel.: 801-581-6078
Fax: 801-581-3357
E-mail: paul.bernstein@hsc.utah.edu

Abstract

The macula of the primate retina uniquely concentrates high amounts of the xanthophyll carotenoids lutein, zeaxanthin, and *meso*-zeaxanthin, but the underlying biochemical mechanisms for this spatial- and species-specific localization have not been fully elucidated. For example, despite abundant retinal levels in mice and primates of a binding protein for zeaxanthin and *meso*-zeaxanthin, the pi-isoform of glutathione S-transferase (GSTP1), only human and monkey retinas naturally contain detectable levels of these carotenoids. We therefore investigated whether or not differences in expression, localization, and activity between mouse and primate carotenoid metabolic enzymes could account for this species-specific difference in retinal accumulation. We focused on β,β-carotene-9',10'-dioxygenase (BCO2; also known as BCDO2), the only known mammalian xanthophyll cleavage enzyme. RT-PCR, western blot analysis, and immunohistochemistry confirmed that BCO2 is expressed in both mouse and primate retinas. Co-transfection of expression plasmids of human or mouse BCO2 into *E. coli* strains engineered to produce zeaxanthin demonstrated that only mouse BCO2 is an active zeaxanthin cleavage enzyme. Surface plasmon resonance (SPR) binding studies showed that the binding affinities between human BCO2 and lutein, zeaxanthin, and *meso*-zeaxanthin are 10- to 40-fold weaker than those for mouse BCO2, implying that ineffective capture of carotenoids by human BCO2 prevents cleavage of xanthophyll carotenoids. Moreover, BCO2 knockout mice, unlike wild-type mice, accumulate zeaxanthin in their retinas. Our results provide a novel explanation for how primates uniquely concentrate xanthophyll carotenoids at high levels in retinal tissue.

Key words: β,β-carotene-9',10'-dioxygenase (BCO2); zeaxanthin; carotenoids; macula; retina; xanthophylls; cleavage; surface plasmon resonance (SPR)

UU IR Author Manuscript

Significance Statement

Among mammals, only primates can accumulate high levels of xanthophyll carotenoids in their retinas. We discovered that unlike most other mammals, the major xanthophyll cleavage enzyme, β,β-carotene-9',10'-dioxygenase (BCO2), is inactive in humans, explaining the unique accumulation of lutein, zeaxanthin, and *meso*-zeaxanthin in the primate macula. We confirmed this discovery by demonstrating that BCO2 knockout mice accumulate zeaxanthin in their retinas.

Author contributions

B.L., W.B., and P.S.B. designed research; B.L., P.P.V., A.G., Z.S., H.S., B.M.B., K.N., M.M.H., and J.M.F. performed research; B.L., P.P.V., W.B., and P.S.B analyzed data; B.L., W.B., and P.S.B wrote the paper.

\body

The macular pigment of the human retina consists of the xanthophyll carotenoids, lutein, zeaxanthin, and their metabolite, *meso*-zeaxanthin (1-3). Macular pigments are highly concentrated in the foveal area of the human retina. Their highest concentration can reach 1 mM, making the macula a visible yellow spot at the center of the human retina. These xanthophylls are known to play antioxidant and light-screening roles in nature (4-6). Clinical studies have shown that lutein and zeaxanthin supplementation can reduce the risk of age-related macular degeneration (AMD), a leading cause of blindness in the developed world (4, 7, 8). Recently, the Age-Related Eye Disease Study 2 (AREDS2) showed that daily oral supplementation with 10 mg of lutein and 2 mg of zeaxanthin was associated with 10%-18% reduced progression to advanced AMD over the 5-year study relative to original AREDS formulations without lutein and zeaxanthin, and the authors recommended adding lutein and zeaxanthin to replace β-carotene in the formulation for safety and efficacy reasons (9, 10).

UU IR Author Manuscript

The spatially and chemically specific accumulation of high concentrations of xanthophylls in the retina is a unique feature of the primate retina relative to other mammals, but the biochemical basis for this high degree of specificity is unclear. High-affinity binding proteins might drive this process. Mice and humans express a zeaxanthin-binding protein, the pi-isoform of glutathione-S-transferase (GSTP1), abundantly in the retina, yet only the human retina naturally contains zeaxanthin and *meso*-zeaxanthin (11, 12). Thus, other biochemical mechanisms underlying accumulation of the human macular pigment need to be considered.

β,β-Carotene-9',10'-dioxygenase (BCO2; also known as BCDO2) is a xanthophyll carotenoid cleavage enzyme which can cleave carotenoids in many animals eccentrically at the 9-10 or 9'-10' carbon-carbon double-bonds into C13- and C27-apo-carotenoids, or further into C14-dialdehyde (13, 14). Its physiological function is supported by genetic evidence from several species. A nonsense mutation in the sheep *BCO2* gene that introduces a stop codon at amino acid 66 of the 575 amino acid full-length protein is strongly associated with a yellow fat phenotype due to the high amount of lutein that deposits in tissue (15). *Cis*-acting and tissue-specific regulatory mutations that inhibit the expression of BCO2 in domestic chickens can cause them to have yellow skin secondary to carotenoid accumulation (16). Genetic variations in the *BCO2* gene have been reported to increase carotenoid levels in bovine adipose tissue and milk (17). *In vitro* biochemical studies have also demonstrated that ferret BCO2 can cleave lutein and zeaxanthin (13).

BCO2, BCO1 and *RPE65* are members of the polyene oxygenase gene family. BCO1, which is also known as BCMO1, cleaves β-carotene symmetrically at the 15-15' position to yield two molecules of retinal, the key pigment in the visual cycle, and it is inactive with xanthophyll (oxygenated) carotenoids such as lutein and zeaxanthin (18, 19). RPE65, an essential enzyme in the visual cycle, participates in the conversion of all-*trans*-retinyl palmitate to 11-*cis*-retinol, and various mutations are associated with Leber's congenital amaurosis type 2 (LCA2) and retinitis

UU IR Author Manuscript

pigmentosa (18, 20-22). BCO2 may also play important roles in ocular tissues, but a physiological function has not been established. Based on the fact that high amounts of lutein and zeaxanthin exist in the human macula, we hypothesized that either human BCO2 is not expressed in human retina, or it is an inactive carotenoid cleavage enzyme. In this study, we tested these proposed hypotheses by investigating the expression, distribution, and activity of BCO2 in human, monkey, and mouse retina.

Results

Expression and Localization of BCO2 in Mammalian Retina. To determine if BCO2 is expressed in the human retina, western blots were performed using an anti-BCO2 antibody. A polypeptide of ~63 kDa was detected in the total protein preparation of human retina (Figure 1a). The human *BCO2* gene expresses five protein splice variants: a, b, c, d and e, which are composed of 579, 545, 539, 506 and 474 amino acids, respectively (NCBI database) which differ only at the N-terminal, and all of which, except for isoform d, preserve the enzymes' active sites. According to the mobility of BCO2 revealed on the western blot, isoforms a, b and c are the most likely candidates. RT-PCR detected the mRNA of isoform a, but not isoforms b or c (Figure 1b). By immunohistochemistry (IHC), BCO2 is localized throughout the monkey retina, especially in the inner segments, inner retina and ganglion cells (Figure 1c). We also examined BCO2's expression in mouse retina and identified a polypeptide of ~63 kDa (Figure 2a) on a western blot with mouse retina lysates. A single amplicon of ~640 bp (Figure 2b) suggested that mouse retina expresses only one BCO2 isoform. As observed in monkey retina, IHC results showed that mouse BCO2 is expressed throughout the retina and retinal pigment epithelium (RPE) (Figure 2c).

Carotenoid Cleavage Assays. Next, we investigated the enzyme activity of human and mouse BCO2 using a cell-based carotenoid cleavage assay. These assays have been employed to test the activity of many carotenoid oxygenases with zeaxanthin, β-carotene, and lycopene (23-28). In our

UU IR Author Manuscript

first experiments, a plasmid of various BCO2 constructs was transfected into a bacterium that had been engineered to carry a zeaxanthin synthesis plasmid. If following transfection, the bacterium remains yellow in color, it indicates that the enzyme is inactive; if the carotenoid coloration disappears, it suggests that the enzyme is a functional enzyme. The yellow color of zeaxanthin was faded in the bacteria transfected with mouse BCO2 plasmids (Figure 3a), demonstrating that mouse BCO2 can cleave zeaxanthin. Human BCO2 isoform a (human BCO2a) failed to cleave zeaxanthin, retaining the yellow color. The cleavage products of each assay were then analyzed by HPLC (Figure 3b). Chromatograms of the human BCO2 experiments are identical to those of the control experiments, consistent with absence of cleavage activity. In the chromatogram of the mouse BCO2 experiment, the elution peak of zeaxanthin almost disappeared, while a new peak appeared at 14.22 minutes whose diode-array spectrum and retention time were consistent with C14-dialdehyde (also known as rosafluene dialdehyde; Figure 3b, inset), a previously reported major cleavage product of zeaxanthin by BCO2 (14). These experiments demonstrate that human retinal BCO2 is an inactive enzyme, while mouse BCO2 is an active carotenoid cleavage enzyme.

Protein Sequence and Structure Analysis. To explain the functional difference between human BCO2 and mouse BCO2, we analyzed the amino acid sequences of human BCO2a and mouse BCO2. Sequence alignments (Figure 4, upper panel) show that the major difference between human BCO2a enzyme and mouse BCO2 is the presence of four amino acid residues, GKAA, in human BCO2 (Figure 4), suggesting loss of an alternate splice site in the human gene. An NCBI protein database search revealed that this GKAA insertion is apparently unique to primates and is absent in cows, sheep, rats, mice, and ferrets. GKAA is also absent in human and mouse RPE65 that can actively cleave all-*trans*-retinyl esters. Inspecting the human and mouse BCO2 genes reveals that GKAA represents an extension of human BCO2 exon 3 caused by use of an alternate donor splice site (Figure S1). Deletion of GKAA between P125 and M127 and replacement of A126 by T are expected to induce a substantial change in structure in this area, but no significant difference is found at their

UU IR Author Manuscript

enzymatic cleavage domains, as all four key histidine residues are conserved (shaded red in Figure 4, upper panel). We also compared the 3-D homology structure of human BCO2a with that of mouse BCO2 using RPE65 crystal structure (PDB 3fsn.1.a) as a template, and we confirmed that there are no significant differences between human BCO2a and mouse BCO2 cleavage domains (Figure 4, lower panel). As expected, the GKAA deletion in the N-terminal half of human BCO2 caused a structural re-arrangement (boxes in Figure 4, lower panel). Next, the activity of human BCO2 enzyme with its GKAA sequence deleted was tested using the cell-based carotenoid cleavage assay to determine if enzymatic activity could be restored. The modified expression vector of human BCO2 in which the nucleotides encoding GKAA were deleted was transfected into *E. coli* carrying a zeaxanthin synthesis plasmid. These bacteria retained their yellow color, indicating that simple deletion of GKAA cannot convert human BCO2 into an active carotenoid cleavage enzyme. Replacing the N-terminal 197 amino acids of human BCO2a with the N-terminal 150 amino acids of mouse BCO2 or substitution of a wide range of amino acid residues of human BCO2 with the corresponding residues of mouse BCO2 could not restore human BCO2's cleavage activity (Figure S2 and Table S1). Conversely, insertion of GKAA into mouse BCO2 inactivates the enzyme, demonstrating that the GKAA insertion alone is sufficient to inactivate mouse BCO2. Further studies in which we combined deletion of GKAA from human BCO2 with several key amino acid substitutions selected from the mouse BCO2 sequence still could not rescue human BCO2's function, implying that there has been considerable genetic drift since primate BCO2 first acquired the GKAA insertion and lost its xanthophyll cleavage function.

Carotenoid Binding Affinity Measurements by Surface Plasmon Resonance (SPR). The 3-D protein structure of an apo-carotenoid cleavage oxygenase (ACO) from the cyanobacterium *Synechocystis sp. PCC6803* demonstrates that a substrate–binding tunnel is present near the cleavage domain (29). Without access to the substrate-binding tunnel, carotenoids cannot be cleaved. This led us to investigate whether or not there is a difference in carotenoid binding

UU IR Author Manuscript

affinities between human and mouse BCO2 by SPR. Figure S3 shows the recombinant proteins used for SPR experiments. Table 1 and Figure S4 show that human BCO2a has much weaker binding affinity for xanthophylls than mouse BCO2. For example, the K_D of *meso*-zeaxanthin to human BCO2a is around 40–fold higher than that of mouse BCO2. These data demonstrate that the binding affinities between xanthophylls and mouse BCO2 are stronger than those associated with human BCO2a, implying that weak binding of carotenoids may be the reason why human BCO2 has lost its cleavage function.

Detection of Zeaxanthin in the Retina of BCO2 Knockout (BCO2$^{-/-}$) Mouse. Finally, we tested if induced inactivity of BCO2 can cause the retinal accumulation of xanthophyll carotenoids by feeding zeaxanthin to BCO2$^{-/-}$ mice. Carotenoid contents were extracted from the retinas, RPE/choroids, and lenses of BCO2 knockout mice, respectively, and zeaxanthin was identified according to zeaxanthin standard's retention time and UV-visible spectrum from HPLC-PDA detectors on two different chromatographic column systems (cyano and chiral) and by mass spectrometry. Figure 5 shows that 0.66 ng of zeaxanthin were detected per BCO2$^{-/-}$ mouse's retinas, while zeaxanthin cannot be detected by HPLC in the retina of WT mice, demonstrating that BCO2 is a key enzyme for preventing xanthophyll accumulation in most mammalian retinas. Zeaxanthin levels in RPE/choroid of BCO2$^{-/-}$ mice are around three times higher than that of the WT mice. No zeaxanthin was detected in the lenses of BCO2$^{-/-}$ mice or WT mice.

Discussion

The yellow pigment of the human retina's *macula lutea* (yellow spot) was first noted by anatomists over two hundred years ago (30), and the pigment was chemically identified to be lutein, zeaxanthin, and *meso*-zeaxanthin about thirty years ago (1). Many clinical studies have already indicated that lutein and zeaxanthin supplementation may reduce the risk of AMD; however, the protective mechanisms and physiological functions of the macular carotenoid

UU IR Author Manuscript

pigments have generally been studied only *in vitro* because no other non-primate mammals accumulate carotenoids at high levels in their retinas. Birds, amphibians, and reptiles accumulate their ocular carotenoids through a distinct mechanism involving xanthophyll esterification to fatty acids. In the past, our laboratory has focused on the identification and characterization of specific binding proteins for lutein, zeaxanthin, and *meso*-zeaxanthin. While these proteins may be required for the uptake and stabilization of these compounds in the human retina, they are not sufficient to explain why xanthophylls are not found in other mammalian retinas because these binding proteins are often found in these animals' retinas, too.

Recent investigations on various mammalian BCO2 enzymes have shown that BCO2 can generally cleave xanthophylls such as lutein and zeaxanthin, and BCO2 mutations can cause the tissues of chickens, cows, and sheep to develop a deep yellow color due to carotenoid deposition. To explain the unique deposition of xanthophyll carotenoids in the primate retina, we hypothesized that either human BCO2 is not expressed in human retina, or it is an inactive carotenoid cleavage enzyme. We found that a ~63 kDa polypeptide was strongly labeled by anti-BCO2 antibodies when probed against human, monkey, or mouse retinal total protein preparations and tissue sections, and RT-PCR also detected mRNA of human and mouse BCO2, demonstrating that BCO2 is expressed in both the human and mouse retina. Subsequently, we employed a cell-based carotenoid cleavage assay which showed that human BCO2 is an inactive carotenoid cleavage enzyme, while mouse BCO2 can clearly cleave zeaxanthin. Our finding that human BCO2 is an inactive carotenoid cleavage enzyme is consistent with other published reports. In an investigation on carotenoid uptake mechanisms, human ARPE-19 cells specifically took up high amounts of xanthophyll carotenoids, but no xanthophyll cleavage products were identified in these cells (31). Moreover, no eccentric cleavage products were detected in human subjects given labeled β-carotene supplements (32, 33). Recent genetic analyses have reported no association between SNPs of human BCO2 and macular pigment optical density (MPOD), also implying that human BCO2 cannot cleave macular pigments

UU IR Author Manuscript

(34). Furthermore, our mouse feeding studies showed that BCO2 knockout mice accumulate zeaxanthin in their retinas, but wild-type mice do not (Figure 5), and our SPR results revealed that the binding affinities between a variety of carotenoids and mouse BCO2 are around 10- to 40-times stronger than those between the same carotenoids and human BCO2, demonstrating that the inability to bind potential substrate carotenoids in the active site may be the reason that human BCO2 is an inactive xanthophyll cleavage enzyme. Persistent expression of BCO2 in the human retina despite lack of carotenoid cleavage activity implies that it may serve an as yet unknown enzymatic and/or regulatory function akin to the retinoid isomerohydrolase activity acquired by its relative in the retinal pigment epithelium, RPE65.

To explore the reasons underlying the difference of enzymatic activities between human and mouse BCO2, we examined their primary structures. Sequence alignment (Figure 4) showed the four key histidine residues responsible for enzyme activity and carotenoid cleavage are conserved. The 3-D homology structures of human and mouse BCO2 show that the insertion of GKAA in human BCO2 unfolds a short β-stranded loop present in mouse BCO2 into a much larger unstructured loop (box in Figure 4, lower panel). As this is the only major structural change between human and mouse BCO2, disruption of this loop may be key in preventing human BCO2 from cleaving zeaxanthin by disrupting access to the substrate binding tunnel, and, indeed, insertion of GKAA into mouse BCO2 inactivated the carotenoid cleavage enzyme. On the other hand, deletion of GKAA from human BCO2, replacement of the N-terminal domain of human BCO2 with mouse BCO2, or various substitutions of mouse BCO2 amino acids into corresponding residues of human BCO2 did not restore cleavage function to human BCO2 alone or in combination with the GKAA deletion. All these data suggest that there has been considerable genetic drift since primate BCO2 became inactive which complicates genetically engineered reconstitution of human BCO2's active site. Further attempts to restore human BCO2 activity should be guided by crystallography, but unfortunately, the 3-D structures of BCO2s have not been solved, and the 3-D structure of the

UU IR Author Manuscript

RPE65's binding site for all-*trans*-retinyl palmitate is not well characterized (35, 36). Solving the crystal structures of human BCO2 and mouse BCO2 will facilitate our understanding of these two enzymes' interactions with xanthophylls.

This work reveals that the inactivity of BCO2 with xanthophylls such as zeaxanthin causes primates to be the only mammals that highly accumulate xanthophyll carotenoids in their retinas. It appears that many, if not all, non-primate mammals break down xanthophylls in ocular and non-ocular tissues, but this alone would not account for the selective uptake and the specific localization of just lutein, zeaxanthin, and *meso*-zeaxanthin in the primate retina when there are around 50 carotenoids in the human diet and 15 to 20 in the serum. Several transport proteins such as SR-B1, ABCA1 and HDL are known to be involved in the process of macular pigment uptake (31, 37-39), and the effects of their regulators, PPAR and ISX, also need to be considered in the carotenoid absorption process (40, 41). During *et al.* reported that SR-B1 is involved in xanthophyll uptake into cultured retinal cells (31). Carotenoid supplementation did not elevate the carotenoid levels in the retina of the WHAM chicken whose ABCA1 transport protein is defective, and many studies have shown a significant positive association between the concentration of serum HDL and that of serum lutein and zeaxanthin. The other known carotenoid cleavage enzyme, BCO1, also could be considered a contributor to this selective uptake process. The expression of human BCO1 was detected in the cytoplasm of most human tissues (18, 21, 24, 42), and enzymatic assays show that BCO1 prefers to cleave the major carotenoids in human serum such as β-carotene, lycopene, and β-cryptoxanthin but not lutein or zeaxanthin (18, 19). Thus, BCO1 can also be considered a participant in the selective targeting of just lutein and zeaxanthin to the human retina. Within the retina itself, the specific binding proteins, StARD3 (lutein) and GSTP1 (zeaxanthin and *meso*-zeaxanthin), appear to drive the spatial localization to the foveal region because the human retinal distribution of these binding proteins matches well with that of the macular carotenoid pigments (12, 43).

In summary, human BCO2 is present in the human retina, but it showed no carotenoid cleavage activity, while mouse BCO2 is clearly an active carotenoid cleavage enzyme. Losing the ability to capture lutein and zeaxanthin efficiently appears to cause human BCO2 to become an inactive xanthophyll carotenoid cleavage enzyme whose other physiological functions in the human retina remain to be elucidated. Thus, inactivity of BCO2 facilitates xanthophyll deposition in the macula of the human and monkey retina.

Materials and Methods

Tissue Procurement and Preparation. Human donor eyes were procured through the Utah Lions Eye Bank in compliance with tenets of the Declaration of Helsinki. Dissection of the globes was performed within 24 h post-mortem on ice and under dim light. Mouse retinas were also harvested under dim light. Human and mouse tissues were washed twice with PBS and homogenized in 10 mM Tris-HCl buffer (pH 7.4) containing 0.2 mM PMSF and 10 μg/mL aprotinin to prepare total protein extracts.

*Western Blots***.** Proteins were separated and transferred to membranes as described before (43). The membranes were washed and incubated overnight with the primary anti-BCO2 antibody (Proteintech Group, Inc., Chicago, IL) at a dilution of 1:5000. The membranes were incubated with horseradish peroxidase-conjugated secondary antibody [1:1000 polyclonal goat anti-rabbit IgG (H+L)-HRP] for 2 h at room temperature. Membranes were developed using ECL Plus Western blot detection reagents (Amersham Biosciences, Pittsburgh, PA).

Reverse Transcription-Polymerase Chain Reaction (RT-PCR). Total RNA (2 μg) was prepared from human retina and mouse retina. cDNA was synthesized using SuperScript II reverse transcriptase (Invitrogen, Carlsbad, CA). PCR amplification was performed using a 1 μL reaction mixture as a template. PCRs were performed using the following primer pairs: human *BCO2a* forward, 5′-AGG AGT CAT TCT GCC ACT GC-3′; and human *BCO2a* reverse, 5′-TCT CTG GAG GAA CCC

UU IR Author Manuscript

GAA TAA CC -3'; human *BCO2b* forward, 5'-GAC ATG GCA ACT GGA TCT TGA AGG -3'; and human *BCO2b* reverse, 5'-TCT CTG GAG GAA CCC GAA TAA CC -3'; human *BCO2c* forward, 5'-ATG GAA CGA TCT GGT GCT CTC ATG-3'; and human *BCO2c* reverse, 5'-TTC TCT CCA AAC CAC ATC AAC C -3'; mouse *BCO2* forward, 5'- TGA CCC ATG CAA GAG CAT CTT TGA ACG -3'; and mouse *BCO2* reverse, 5'-AGC CCT GGT CCT CAA AGG CAT TGA TTT G -3'. Products were evaluated by electrophoresis on an ethidium bromide-stained 1% agarose gel in 1× TBE buffer. The amplicons were cloned and sequenced for verification.

Immunohistochemistry (IHC). Confocal microscope images were derived from a *Macaca mulatta* monkey or from mouse eyes as described earlier (43). Monkey retinas were chosen because of the availability of high quality perfusion-fixed tissue and the 96% homology of human and monkey BCO2. Shortly after fixation, cryosections (12 μm thick) were cut, rinsed in 0.1 M phosphate buffer containing 0.1% Triton X-100 (PBT), and blocked for 1 h using 10% normal donkey serum in PBT. Antibodies directed against human BCO2 (1:2000 dilution) or mouse BCO2 (1:2000 dilution) were applied overnight at 4 °C. After the samples had been rinsed in PBT (3 × 10 min FITC-conjugated secondary antibodies (Jackson ImmunoResearch Laboratories, West Grove, PA) were applied for 2 h at room temperature. Immunolocalization was imaged using a Zeiss LSM 510 confocal microscope set to an optical slice of <0.9 μm. Control sections, which were not incubated in primary antibodies, were processed in parallel and found to be negative.

Carotenoid Cleavage Assays. The expression vectors, EX-Z2826-B05 (human BCO2a) and EX-Mm13746-B05 (mouse BCO2), were purchased from GeneCopoeia (Rockville, MD). The cDNAs were cloned into pReceiver-B05 vector with a Tac promoter, N-GST tag, and TEV protease site. EX-NEG-B05 (Empty pReceiver-B05) was used as a negative control. All three vectors were transformed into *E. coli* BL21 carrying an expression plasmid for zeaxanthin biosynthesis (44, 45). The transformed *E. coli* were grown overnight at 37°C on LB solid medium containing 100 μg/ml of

UU IR Author Manuscript

ampicillin and 35 μg/ml of chloramphenicol. Selected colonies were picked into 5 ml of LB medium containing 100 μg/ml of ampicillin and 35 μg/ml of chloramphenicol and grown at 37°C with shaking until the OD_{600} was 0.5-0.7. Then, protein expression was induced by adding IPTG to a final concentration of 1 mM. After growing the cultures for an additional 3-5 h, they were then streaked on the same LB solid medium and incubated at 25°C for 2-3 days in darkness. In this system, carotenoid cleavage activity is visualized qualitatively by the lack of accumulating carotenoids which results in the absence of the yellow color characteristic of the control cells containing carotenoid synthesis enzymes but no cleavage enzymes. The bacteria on the plates were collected for HPLC analysis to confirm the presence of typical carotenoid cleavage products such as C14-dialdehyde. The extracted carotenoid contents were dried and re-dissolved in the HPLC mobile phase. HPLC separation was carried out on a C30 column (YMC Europe GmbH, Dinslaken, Germany; 25 cm length 4.6 mm i.d.) as before (46).

In order to try to restore the carotenoid cleavage activity of human BCO2, substitution of amino acid residues of human BCO2 with the corresponding residues of mouse BCO2 was performed according to Figure S2 and Table S1. All the chimera constructs were generated using human BCO2a, human BCO2b, or mouse BCO2 expression vectors as templates, respectively. All the primers as shown in Table S1 were designed using QuikChange® Primer Design Program of Agilent Technologies. The mutagenesis experiments were carried out by QuickChange II XL Site-Directed Mutagenesis Kit or QuickChange Multi Site-Directed Mutagenesis Kit (Agilent Technologies). After confirmation by DNA sequencing, all the constructs were co-transfected with the zeaxanthin synthesis plasmid into BL21 to assay for carotenoid cleavage activity as described above.

Surface Plasmon Resonance (SPR) Binding Studies. SPR analyses were conducted as before (47, 48). Briefly, the proteins (human BCO2a, mouse BCO2 and human serum albumin (HSA)) at 10-50 μg/ml in 10 mM sodium acetate (pH 5.0) were immobilized on the sensor chip surface using

UU IR Author Manuscript

standard amine-coupling to obtain a density of 10-12 kRU. Each of the three carotenoids was dissolved in DMSO to achieve a high concentration, and 10 mM 4-(2-hydroxyethyl)-1-piperazineethanesulfonic acid (HEPES pH 7.4) with 0.01% Tween-20 and 3% DMSO was used as the running buffer. Typically, the analyte concentration series spanned 0.01–50 μM. Five of these blanks were analyzed at the beginning of the analysis, and the remaining blanks were interspersed throughout the analysis for double-referencing purposes. Each of the analytes was run in triplicate. The analyte concentration series was injected as two-fold dilutions (seven dilutions) in running buffer using the FastStep™ gradient injection mode.

3-D Structure of BCO2s. Using RPE65 (PDB 3fsn.1.a) as their templates, the protein homology structures of human and mouse BCO2 were prepared through PyMol (Schrödinger, LLC, Portland, Oregon).

Mouse Feeding Studies. Twenty five three-month-old BCO2 knockout ($BCO2^{-/-}$) mice (bred at the University of Utah vivarium using founders from Case Western Reserve University), and twenty five three–month-old wild type (WT) C57/BL6 mice were fed with DSM ActiLease zeaxanthin beadlets mixed with their chow (~2.6 mg per mouse per day) for four weeks after first receiving a vitamin A deficient chow (AIN-93) for four weeks to help promote carotenoid uptake. Retinas, RPE/choroid, and lenses of the mice from each feeding group were pooled together in batches of five pairs of tissue, respectively. Zeaxanthin levels in the mouse ocular tissues were analyzed by HPLC on a cyano column (Microsorb 250 mm x 4.6 mm, Rainin Instrument Co. Woburn, WA, USA) as before (49) with confirmation of identity by retention time and UV/visible spectrum, and mass spectrum versus authentic zeaxanthin standard. Chiral HPLC analysis confirmed the presence of *3R,3'R*-zeaxanthin and absence of *3R,3'S-meso*-zeaxanthin.

Acknowledgements:

UU IR Author Manuscript

We thank Dr. Francis Cunningham from the University of Maryland for the kind gift of plasmids to produce carotenoid-accumulating *E. coli* stains. We also thank Dr. Johannes von Lintig of Case Western Reserve University for kindly providing the BCO2 knockout mice and critical reading of the manuscript. This work was supported by grants from the National Eye Institute (EY-11600 and EY-14800), Kemin Health (Des Moines, Iowa), and by unrestricted grants to the University of Utah, Department of Ophthalmology, from Research to Prevent Blindness (RPB; New York). WB is the recipient of a Research to Prevent Blindness Senior Investigator Award.

References:

1. R. A. Bone, J. T. Laudrum, & Tarsis SL (1985) Preliminary identification of the human macular pigment. *Vis. Res* 25:1531-1535.
2. Bone RA & Landrum JT (1984) Macular pigment in Henle fiber membranes: a model for Haidinger's brushes. *Vision Res.* 24:103-108.
3. F. Khachik, P. S. Bernstein, & Garland DL (1997) Identification of lutein and zeaxanthin oxidation products in human and monkey retinas. *Invest. Ophthalmol. Vis. Sci.* 38:1802-1811.
4. Beatty S, Boulton M, Henson D, Kon H-H, & Murray IJ (1999) Macular pigment and age relate macular degeneration. *Br. J. Ophthalmol.* 83:867-877
5. N. I. Krinsky, J. T. Landrum, & Bone RA (2003) Biologic mechanisms of the protective role of lutein and zeaxanthin in the eye. *Annu. Rev. Nutr.* 23:171-201.
6. Whitehead AJ, Mares JA, & Danis RP (2006) Macular pigment. *Arch. Ophthalmol.* 124:1038-1045.
7. R. A. Bone, *et al.* (2001) Macular pigment in donor eyes with and without AMD: a case-control study. *Invest Ophthalmol Vis Sci.* 42:235-240.

8. J. T. Landrum, *et al.* (1997) A one year study of the macular pigment: the effect of 140 days of a lutein supplement. *Exp. Eye Res.* 65:57-62.

9. Chew EY, *et al.* (2013) Secondary Analyses of the Effects of Lutein/Zeaxanthin on Age-Related Macular Degeneration Progression: AREDS2 Report No. 3. *JAMA Ophthalmol*.

10. Chew EY, *et al.* (2013) Lutein/zeaxanthin for the treatment of age-related cataract: AREDS2 randomized trial report no. 4. *JAMA Ophthalmol* 131(7):843-850.

11. Yu H, *et al.* (2013) Dietary wolfberry upregulates carotenoid metabolic genes and enhances mitochondrial biogenesis in retina of db/db diabetic mice. *Mol Nutr Food Res* 57(7):1158-1169.

12. P. Bhosale, *et al.* (2004) Identification and characterization of a pi isoform of glutathione S-transferase as a zeaxanthin-binding protein in the macula of the human eye. *J. Biol. Chem.* 279:49447-49454.

13. Mein JR, Dolnikowski GG, Ernst H, Russell RM, & Wang XD (2011) Enzymatic formation of apo-carotenoids from the xanthophyll carotenoids lutein, zeaxanthin and beta-cryptoxanthin by ferret carotene-9',10'-monooxygenase. *Arch Biochem Biophys* 506(1):109-121.

14. Amengual J, *et al.* (2011) A mitochondrial enzyme degrades carotenoids and protects against oxidative stress. *FASEB J* 25(3):948-959.

15. Vage DI & Boman IA (2010) A nonsense mutation in the beta-carotene oxygenase 2 (BCO2) gene is tightly associated with accumulation of carotenoids in adipose tissue in sheep (Ovis aries). *BMC Genet* 11:10.

16. Eriksson J, *et al.* (2008) Identification of the yellow skin gene reveals a hybrid origin of the domestic chicken. *PLoS Genet* 4(2):e1000010.

UU IR Author Manuscript

17. Tian R, Pitchford WS, Morris CA, Cullen NG, & Bottema CD (2010) Genetic variation in the beta, beta-carotene-9', 10'-dioxygenase gene and association with fat colour in bovine adipose tissue and milk. *Anim Genet* 41(3):253-259.

18. Lindqvist A & Andersson S (2002) Biochemical properties of purified recombinant human beta-carotene 15,15'-monooxygenase. *J Biol Chem* 277(26):23942-23948.

19. Dela Sena C, *et al.* (2013) Substrate Specificity of Purified Recombinant Human beta-Carotene 15,15'-Oxygenase (BCO1). *J Biol Chem* 288(52):37094-37103.

20. Fierce Y, *et al.* (2008) In vitro and in vivo characterization of retinoid synthesis from beta-carotene. *Arch Biochem Biophys* 472(2):126-138.

21. Hessel S, *et al.* (2007) CMO1 deficiency abolishes vitamin A production from beta-carotene and alters lipid metabolism in mice. *J Biol Chem* 282(46):33553-33561.

22. Boulanger A, *et al.* (2003) Identification of beta-carotene 15, 15'-monooxygenase as a peroxisome proliferator-activated receptor target gene. *FASEB J* 17(10):1304-1306.

23. Kiefer C, *et al.* (2001) Identification and characterization of a mammalian enzyme catalyzing the asymmetric oxidative cleavage of provitamin A. *J Biol Chem* 276(17):14110-14116.

24. Redmond TM, *et al.* (2001) Identification, expression, and substrate specificity of a mammalian beta-carotene 15,15'-dioxygenase. *J Biol Chem* 276(9):6560-6565.

25. Schwartz SH, Qin X, & Zeevaart JA (2001) Characterization of a novel carotenoid cleavage dioxygenase from plants. *J Biol Chem* 276(27):25208-25211.

26. Sun Z, *et al.* (2008) Cloning and characterisation of a maize carotenoid cleavage dioxygenase (ZmCCD1) and its involvement in the biosynthesis of apocarotenoids with various roles in mutualistic and parasitic interactions. *Planta* 228(5):789-801.

UU IR Author Manuscript

27. Schwartz SH, Qin X, & Loewen MC (2004) The biochemical characterization of two carotenoid cleavage enzymes from Arabidopsis indicates that a carotenoid-derived compound inhibits lateral branching. *J Biol Chem* 279(45):46940-46945.

28. Garcia-Limones C, *et al.* (2008) Functional characterization of FaCCD1: a carotenoid cleavage dioxygenase from strawberry involved in lutein degradation during fruit ripening. *J Agric Food Chem* 56(19):9277-9285.

29. Kloer DP & Schulz GE (2006) Structural and biological aspects of carotenoid cleavage. *Cell Mol Life Sci* 63(19-20):2291-2303.

30. Home E (1798) An account of the orifice in the retina of the human eye, discovered by Professor Soemmering: to which are added proofs of this appearance being extended to the eyes of other animals. *Philos Trans R Soc Lond* 2:332-345.

31. A. During, S. Doraiswamy, & Harrison EH (2008) Xanthophylls are preferentially taken up compared with beta-carotene by retinal cells via a SRBI-dependent mechanism. *J Lipid Res* 49:1715-1724.

32. Krinsky NI, Wang XD, Tang G, & Russell RM (1993) Mechanism of carotenoid cleavage to retinoids. *Ann N Y Acad Sci* 691:167-176.

33. Yeum KJ & Russell RM (2002) Carotenoid bioavailability and bioconversion. *Annu Rev Nutr* 22:483-504.

34. Meyers KJ, *et al.* (2013) Genetic determinants of macular pigments in women of the Carotenoids in Age-Related Eye Disease Study. *Invest Ophthalmol Vis Sci* 54(3):2333-2345.

35. Kiser PD, Golczak M, Lodowski DT, Chance MR, & Palczewski K (2009) Crystal structure of native RPE65, the retinoid isomerase of the visual cycle. *Proc Natl Acad Sci U S A* 106(41):17325-17330.

36. Chander P, Gentleman S, Poliakov E, & Redmond TM (2012) Aromatic residues in the substrate cleft of RPE65 protein govern retinol isomerization and modulate its progression. *J Biol Chem* 287(36):30552-30559.

37. Connor WE, Duell PB, Kean R, & Wang Y (2007) The prime role of HDL to transport lutein into the retina: evidence from HDL-deficient WHAM chicks having a mutant ABCA1 transporter. *Invest Ophthalmol Vis Sci* 48(9):4226-4231.

38. Yu Y, *et al.* (2011) Association of variants in the LIPC and ABCA1 genes with intermediate and large drusen and advanced age-related macular degeneration. *Invest Ophthalmol Vis Sci* 52(7):4663-4670.

39. E. Loane, *et al.* (2008) Transport and retinal capture of lutein and zeaxanthin with reference to age-related macular degeneration. *Surv Ophthalmol* 53:68-81.

40. Lobo GP, *et al.* (2013) Genetics and diet regulate vitamin A production via the homeobox transcription factor ISX. *J Biol Chem* 288(13):9017-9027.

41. Desvergne B & Wahli W (1999) Peroxisome proliferator-activated receptors: nuclear control of metabolism. *Endocr Rev* 20(5):649-688.

42. Bhatti RA, *et al.* (2003) Expression of beta-carotene 15,15' monooxygenase in retina and RPE-choroid. *Invest Ophthalmol Vis Sci* 44(1):44-49.

43. Li B, Vachali P, Frederick JM, & Bernstein PS (2011) Identification of StARD3 as a lutein-binding protein in the macula of the primate retina. *Biochemistry* 50(13):2541-2549.

44. Cunningham FX, Jr., Sun Z, Chamovitz D, Hirschberg J, & Gantt E (1994) Molecular structure and enzymatic function of lycopene cyclase from the cyanobacterium Synechococcus sp strain PCC7942. *Plant Cell* 6(8):1107-1121.

45. Cunningham FX, Jr., *et al.* (1996) Functional analysis of the beta and epsilon lycopene cyclase enzymes of Arabidopsis reveals a mechanism for control of cyclic carotenoid formation. *Plant Cell* 8(9):1613-1626.

46. Bhosale P, Serban B, Zhao da Y, & Bernstein PS (2007) Identification and metabolic transformations of carotenoids in ocular tissues of the Japanese quail Coturnix japonica. *Biochemistry* 46(31):9050-9057.

47. Rich RL, Quinn JG, Morton T, Stepp JD, & Myszka DG (2010) Biosensor-based fragment screening using FastStep injections. *Anal Biochem* 407(2):270-277.

48. Vachali P, Li B, Nelson K, & Bernstein PS (2012) Surface plasmon resonance studies on the interactions of carotenoids and their binding proteins. *Arch Biochem Biophys* 519(1):32-37.

49. Li B, Ahmed F, & Bernstein PS (2010) Studies on the singlet oxygen scavenging mechanism of human macular pigment. *Arch Biochem Biophys* 504(1):56-60.

UU IR Author Manuscript

Figure legends:

Figure 1. Expression of BCO2 in the human retina and localization in monkey retina. (a) Western blot of human retina lysates probed with anti-BCO2. The BCO2 polypeptide has a mobility of approximately 65 kDa (calc. MW = 65,674 for the BCO2a isoform). (b) RT-PCR with human retina cDNA and isoform-specific oligonucleotide primers. Human *BCO2* isoform a (1), but not isoform b (2) or isoform c (3), could be identified. (c) Immunohistochemistry of perfusion-fixed monkey retina cryosection probed with antibody directed against BCO2 (green). Propidium iodide (red) permits visualization of nuclear layers. Abbreviations: IS, inner segment layer; ONL, outer nuclear layer; OPL, outer plexiform layer; INL, inner nuclear layer; IPL, inner plexiform layer; GCL, ganglion cell layer. Scale bar = 20 μm.

Figure 2. Expression and localization of BCO2 in the mouse retina. (a) Western blot of mouse retina lysate with anti-mouse BCO2 antibody. The mobility of the mouse BCO2 polypeptides is approximately 60 kDa (calc. MW = 60,142). (b) RT-PCR with mouse *BCO2*-specific primers and mouse retina cDNA. (C) Immunohistochemistry of albino mouse retina cryosection probed with polyclonal anti-BCO2 antibody (green) and contrasted with propidium iodide (red) which binds nucleic acids. Labeling of retina and retinal pigment epithelium (RPE) is specific, as it was absent in the negative control (omission of primary antibody). Scale bar = 20 μm.

Figure 3. Enzymatic activity assays of human and mouse BCO2. (a) Expression of human, mouse *BCO2* cDNA, or empty expression vector in *E. coli* strains engineered for zeaxanthin production. Yellow color indicates absence of enzymatic cleavage activity. White color demonstrates cleavage of zeaxanthin. (b) HPLC analysis on a cyano column of extracts from *E. coli* engineered to synthesize zeaxanthin which had been co-transformed with BCO2 or control vectors (blue trace, mouse BCO2; red trace, human BCO2a; green trace, control; inset, absorption spectra of a cleavage product). Identity of zeaxanthin was confirmed by comparison with photodiode-array spectra and by co-

UU IR Author Manuscript

elution with authentic standard. The photodiode-array spectrum of the peak labeled as C14-dialdehyde (rosafluene dialdehyde) was consistent with a previous report of a major cleavage product of zeaxanthin by mouse BCO2 (14). Retention times of the late eluting peaks are slightly offset due to variations in HPLC chromatographic conditions.

Figure 4. Sequence and structure alignment of human and mouse BCO2. Upper panel, alignment of human BCO2 isoform a, mouse BCO2, and human RPE65 amino acid sequences. Histidine residues that coordinate the iron required for activity in RPE65 are shaded red; hatched box denotes the deletion of GKAA in mouse BCO2. Lower panel, comparison of 3D structures of (A) human BCO2a (green) and mouse BCO2 (cyan), and (B) chimeric human BCO2 (green) and mouse BCO2 (cyan). The boxes identify the structural differences between human BCO2a and mouse BCO2. Histidine residues (blue in human, white in mouse BCO2) coordinating iron (orange) in human and mouse BCO2s are shown as spheres in the center of BCO2.

Figure 5. Zeaxanthin levels in the ocular tissues of BCO2 knockout ($BCO2^{-/-}$) and wild type (WT) mice. Zeaxanthin contents in lens (blue), retina (red) and RPE/choroid (green) were measured by normal phase HPLC; n.d., not detectable. Each experiment was repeated five times on batches of five mice. Error bars represent standard deviations (SD).

Table 1 Equilibrium dissociation constants (K_D) determined by surface plasmon resonance (SPR)

	Human BCO2a (μM)	Mouse BCO2 (μM)	Human Serum Albumin (μM)
Lutein	25.00 ± 2.00	1.17 ± 0.02	2.40± 0.20
Zeaxanthin	19.00 ± 2.00	1.39 ± 0.03	2.20 ± 0.20
meso-Zeaxanthin	46.00 ± 4.00	1.10 ± 0.02	4.50± 0.40

Fig. 1

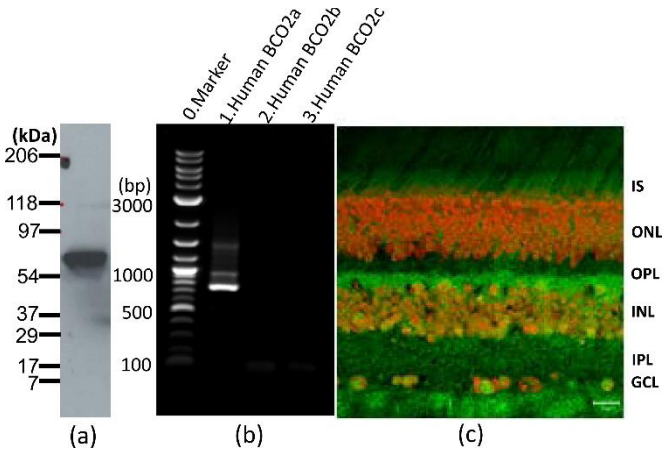
0.Marker
1.Human BCO2a
2.Human BCO2b
3.Human BCO2c
(kDa)
206
118
97
54
37
29
17
7
(bp)
3000
1000
500
100
IS
ONL
OPL
INL
IPL
GCL
(a)
(b)
(c)

Fig. 2

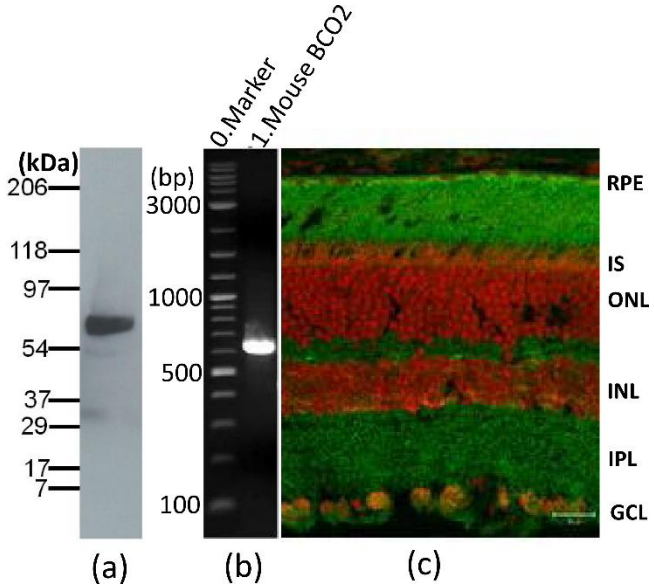
0.Marker
1.Mouse BCO2
(kDa)
206
118
97
54
37
29
17
7
(bp)
3000
1000
500
100
RPE
IS
ONL
INL
IPL
GCL
(a)
(b)
(c)

Fig. 3

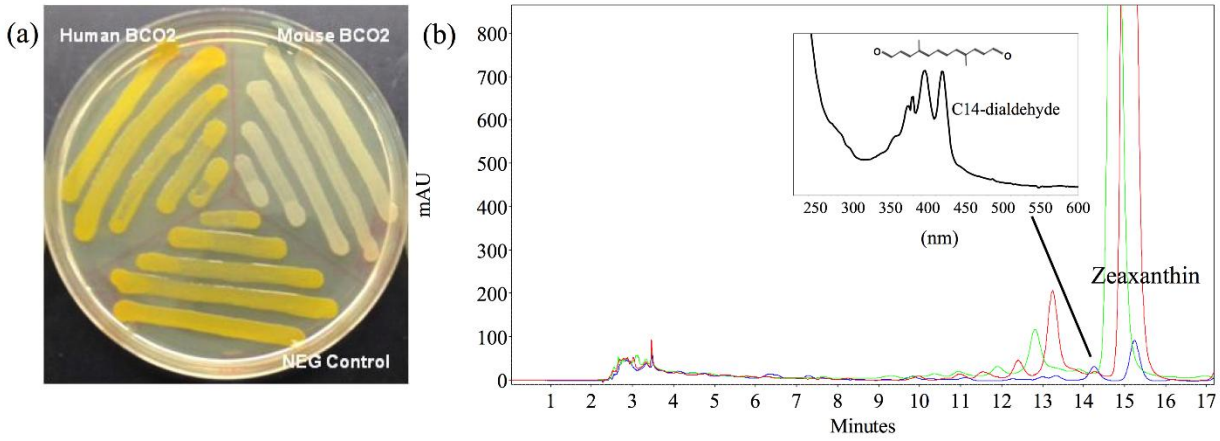
(a)
Human BCO2
Mouse BCO2
NEG Control
(b)
mAU
800
700
600
500
400
300
200
100
0
1 2 3 4 5 6 7 8 9 10 11 12 13 14 15 16 17
Minutes
C14-dialdehyde
250 300 350 400 450 500 550 600
(nm)
Zeaxanthin

Fig. 4

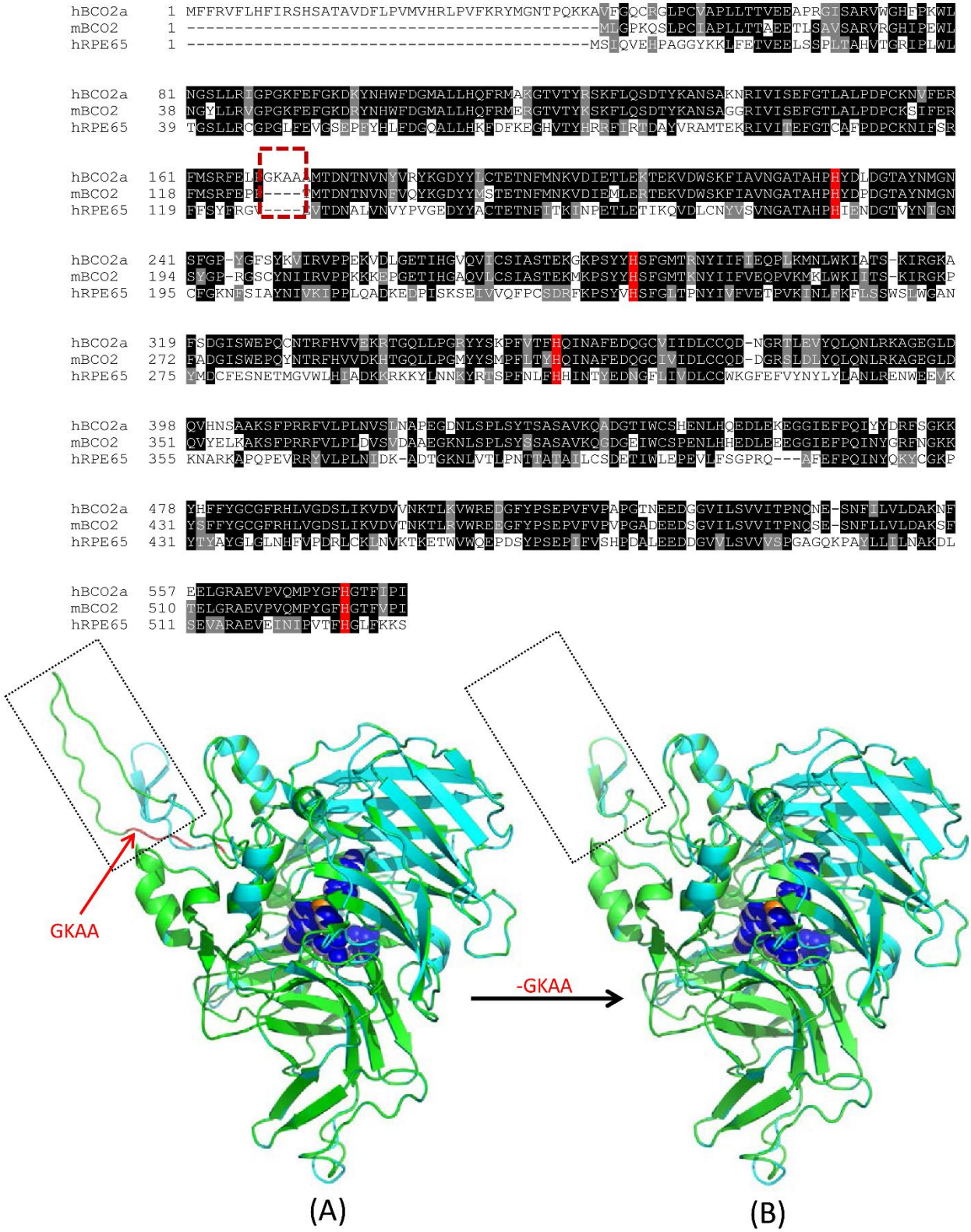
hBCO2a 1 MFFRVFLHFIRSHSATAVDFLPVMVHRLPVFKRYMGNTPQKKAVFGQCRGLPCVAPLLTTVEEAPRGISARVWGHFPKWL
mBCO2 1 ----------MLGPKQSLPCIAPLLTTAEETLSAVSARVRGHIPEWL
hRPE65 1 ----------MSIQVEHPAGGYKKLFETVEELSSPLTAHVTGRIPLWL
hBCO2a 81 NGSLLRIGPGKFEFGKDKYNHWFDGMALLHQFRMAKGTVTYRSKFLQSDTYKANSAKNRIVISEFGTLALPDPCKNVFER
mBCO2 38 NGMLLRVGPGKFEFGKDRYNHWFDGMALLHQFRMEGTVTYKSKFLQSDTYKANSAGGRIVISEFGTLALPDPCKSIFER
hRPE65 39 TGSLLRCGPGLEEVGSEPEYHLFDGQALLHKFDFKEGHVTYHRRFIRTDAYVRAMTEKRIVITEFGTCAFPDPCKNIFSR
hBCO2a 161 FMSRFELLGKAAAMTDNTNVNYVRYKGDYYLCTETNFMNKVDIETLEKTEKVDWSKFIAVNGATAHPHYDLDGTAYNMGN
mBCO2 118 FMSRFEPI-----MTDNTNVNFVQYKGDYYMSTETNFMNKVDIEMLERTEKVDWSKFIAVNGATAHPHYDFDGTAYNMGN
hRPE65 119 FFSYFRGV-----VTDNAIVNVYPVGEDYYACTETNFITKINPETLETIKQVDLCNYVSVNGATAHPHIENDGTVYNIGN
hBCO2a 241 SFGP-YGFSYKVIRVPPEKVDLGETIHGVQVICSIASTEKGKPSYYHSFGMTRNYIIFIEQPLKMNLWKIATS-KIRGKA
mBCO2 194 SYGP-RGSCYNIIRVPPKKKEPGETIHGAQVLCSIASTEKMKPSYYHSFGMTKNYIIFVEQPVKMKLWKIITS-KIRGKP
hRPE65 195 CFGKNFSIAYNIVKIPPLQADKEDPISKSEIVVQFPCSDRFKPSYVHSFGITPNYIVFVETPVKINLFKFLSSWSLWGAN
hBCO2a 319 FSDGISWEPQQNTRFHVVDKRTGQLLPGRYYSKPFVTFHQINAFEDQGCVIIDLCCQD-NGRTLEVYQLQNLRKAGEGLD
mBCO2 272 FADGISWEPQYNTRFHVVDKHTGQLLPGMYYSMPFLTYHQINAFEDQGCIVIDLCCQD-DGRSLDLYQLQNLRKAGEGLD
hRPE65 275 YMDCFESNETMGVWLHIADKKRKKYLNNKYRTSPFNLFHHINTYEDNGFLIVDLCCWKGFEFVYNYLYLANLRENWEEVK
hBCO2a 398 QVHNSAAKSFPRRFVLPLNVSLNAPEGDNLSPLSYTSASAVKQADGTIWCSHENLHQEDLEKEGGIEFPQIYYDRFSGKK
mBCO2 351 QVYELKAKSFPRRFVLPLDVSVDAAEGKNLSPLSYSSASAVKQGDGEIWCSPENLHHEDLEEGGIEFPQINYGRFNGKK
hRPE65 355 KNARKAPQPEVRRYVLPLNIDK-ADTGKNLVTLPNTTATAILCSDETIWLEPEVLFSGPRQ---AFEFPQINYQKYCGKP
hBCO2a 478 YHFFYGCGFRHLVGDSLIKVDVVNKTLKVWREDGFYPSEPVFVPAPGTNEEDGGVILSVVITPNQNE-SNFLLVLDAKNF
mBCO2 431 YSFFYGCGFRHLVGDSLIKVDVTNKTLEVWREEGFYPSEPVFVPVPGADEEDSGVILSVVITPNQSE-SNFLLVLDAKSF
hRPE65 431 YTYAYGLGLNHFVPDRLCKLNVKTKETWVWQEPDSYPSEPIFVSHPDALEEDDGVVLSVVVSPGAGQKPAYLLILNAKDL
hBCO2a 557 EELGRAEVPVQMPYGFHGTFIPI
mBCO2 510 TELGRAEVPVQMPYGFHGTFVPI
hRPE65 511 SEVARAEVEINIPVTFHGLFKKS
GKAA
-GKAA
(A)
(B)

Fig. 5

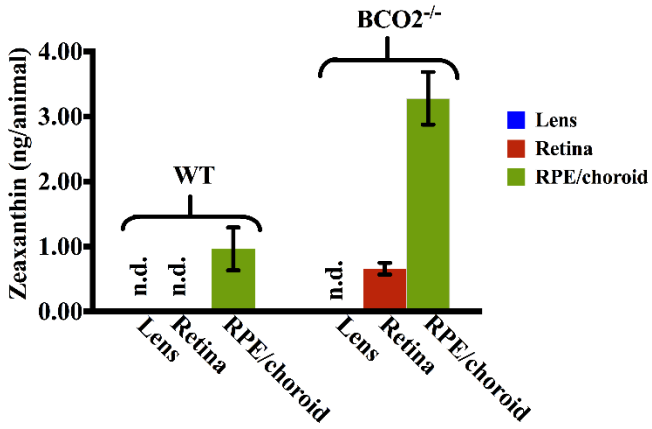
BCO2-/-
WT
Zeaxanthin (ng/animal)
4.00
3.00
2.00
1.00
0.00
n.d.
n.d.
n.d.
Lens
Retina
RPE/choroid
Lens
Retina
RPE/choroid
Lens
Retina
RPE/choroid

Supplementary figure legends

Figure S1. Splice junctions of exon 3/intron 3 and intron 3/exon 4 of the human and mouse BCO2 genes. The insertion of GKAA in the human gene is caused by a change in the donor splice site in the human gene. Intron sequences are in lower case, 5' and 3'-ends are printed in red.

Figure S2. Protein sequences of human BCO2 and mouse BCO2 used to design primers of mutagenesis experiments. Green underline shows the fragments switched between human BCO2 and mouse BCO2, vertical line shows the connection position. Blue underlines show the substituted amino acid positions between human BCO2 and mouse BCO2, and they were numbered. Corresponding numbers were given to the primers in Table S1.

Figure S3. SDS-PAGE (a) and Western blot (b) of recombinant human BCO2a (1), and mouse BCO2 (2) used for SPR.

Figure S4. SPR sensor grams of carotenoids with human BCO2a, mouse BCO2, and human serum albumin (HSA).

Table S1. Primers used in the mutagenesis experiments to restore the carotenoid cleavage function of human BCO2

1. T171M+k174R	5'-aaatttgctccaatctacctttttctgttctttccagcatttcaatgtccactttattcataaagttg-3' 5'-caactttatgaataaagtggacattgaaatgctggaaagaacagaaaaggtagattggagcaaattt-3'
2. L197P	5'-cacatcctcattatgacccggatggaacagcatacaa-3' 5'-ttgtatgctgttccatccgggtcataatgaggatgtg-3'
3. F208Y,Y211R,F213S, S214C, K216N,V217I	5'-ccttctctggaggaacccgaataatattatagcagctaccacgtggcccataggagttccccatattgtatgctg-3' 5'-cagcatacaatatggggaactcctatgggccacgtggtagctgctataatattattcgggttcctccagagaagg-3'
4. E223K,V225K,D226E,L227P	5'-ggattgtctccccaggctccttcttctttggaggaacccgaataaccttatagga-3' 5'-tcctataaggttattcgggttcctccaaagaagaaggagcctggggagacaatcc-3'
5. V234,I237L	5'-agaagcaatagaacataacacctgggctccatggattgtctcc-3' 5'-ggagacaatccatggagcccaggtgttatgttctattgcttct-3'
6. G246M	5'-aaagctatggtagtaagaaggtttcattttctctgtagaagcaatagaacat-3' 5'-atgttctattgcttctacagagaaaatgaaaccttcttactaccatagcttt-3'
7. R258K	5'-gttgttcaatgaaaattatatagttctttgtcattccaaagctatggtagtaa-3' 5'-ttactaccatagctttggaatgacaaagaactatataattttcattgaacaac-3'
8. I264V, L268V, N271K,A276I	5'-ctttccccgaattttagaagtgataattttccacaggttcatctttagag-3' 5'-gttcatctttagaggttgttcaacgaaaattatatagttccttgtcattc-3' 5'-tagaagtggcaattttccacagcttcatctttacaggttgttcaatgaaaattata-3' 5'-tataattttcattgaacaacctgtaaagatgaagctgtggaaaattgccacttcta-3' 5'-gaatgacaaggaactatataattttcgttgaacaacctctaaagatgaac-3' 5'-ctctaaagatgaacctgtggaaaattatcacttctaaaattcggggaaag-3'
9. A284P,S286A	5'-ccagcttatcccatctgcaaagggctttccccgaattttag-3' 5'-ctaaaattcggggaaagccctttgcagatgggataagctgg-3'

10. C295Y	5'-catgaaaccgcgtattatactggggttcccagctt-3' 5'-aagctgggaaccccagtataatacgcggtttcatg-3'
11. E303D, R305H	5'-gaaggagctgtccagtgtgtttatccaccacatgaaaccg-3' 5'-cggtttcatgtggtggataaacacactggacagctccttc-3'
12. R313M, K317M, V320L, F322Y	5'-aaaggcattgatttgatgatatgtaagaaaaggcatgctgtagtacatccctggaaggagctgtccagt-3' 5'-actggacagctccttccagggatgtactacagcatgccttttcttacatatcatcaaatcaatgccttt-3'
13. V334I, I335V	5'-ttgacagcacaaatcaattacaatacagccctggtcctcaaagg-3' 5'-cctttgaggaccagggctgtattgtaattgatttgtgctgtcaa-3'
14. N343D, T346S, E348D,V349L	5'-ctgagattctgtaactggtaaagatctaggcttcttccatcatcttgacagcacaaatcaatt-3' 5'-aattgatttgtgctgtcaagatgatggaagaagcctagatctttaccagttacagaatctcag-3'
15. H366Y, N367E, S368L,A369K	5'-caaaccttcgagggaaagatttggcttttaactcatagacctgatcaagcccttccccagcct-3' 5'-aggctggggaagggcttgatcaggtctatgagttaaaagccaaatctttccctcgaaggtttg-3'
16. N382D, L385V, N386D, P388A, D391K	5'-tcgaaggtttgttttgcctttagatgtcagtgtggatgccgctgagggaaagaacctgagtcca-3' 5'-tggactcaggttctttccctcagcggcatccacactgacatctaaaggcaaaacaaaccttcga-3'
17. T399S	5'-cagcactggctgaagaataggacaatggactcagg-3' 5'-cctgagtccattgtcctattcttcagccagtgctg-3'
18. A407G, T410E, H415P,Q420H, K425E	5'-caatgcctccttcctcttctaggtcctcctgatgt-3' 5'-acatcaggaggacctagaagaggaaggaggcattg-3' 5'-tctcatgaaaatctacatcatgaggacctagaaaaggaagg-3' 5'-gaacgatctggtgctctcctgaaaatctacatcagga-3' 5'-cagtgctgtgaaacagggtgatggagagatctggtgctctcatg-3' 5'-catgagagcaccagatctctccatcaccctgtttcacagcactg-3' 5'-ccttcctttctaggtcctcatgatgtagattttcatgaga-3' 5'-tcctgatgtagattttcaggagagcaccagatcgttc-3'
19. Y435N, D437G, S440N, H445S	5'-ccacagccataaaagaaactatacttttgccactgaatcgatcatagtagat-3' 5'-atctactatgatcgattcagtggcaaaaagtatagtttcttttatggctgtgg-3' 5'-aaaagaaatgatacttttgccattgaatcgaccatagttgatctgaggaaattcaatgcctc-3' 5'-gaggcattgaatttcctcagatcaactatggtcgattcaatggcaaaaagtatcatttctttt-3'

20. V466T, K471R, D476E	5'-gagggataaaagccctcttctctccaaaccttcagtg-3' 5'-ccaaaccttcagtgtcttattcgtcacatcaaccttgatcagagaa-3' 5'-ttctctccaaaccctcagtgtcttattcaccacatcaac-3' 5'-ttctctgatcaaggttgatgtgacgaataagacactgaaggtttgg-3' 5'-cactgaaggtttggagagaagagggcttttatccctc-3' 5'-gttgatgtggtgaataagacactgagggtttggagagaa-3'
21. A488V, T491A, N492D, G496S	5'-agaataaccccactatcttcttcattggttcctggtgc-3' 5'-cccaccatcttcttcatcggctcctggtactggaacaaaaacaggt-3' 5'-gcaccaggaaccaatgaagaagatagtggggttattct-3' 5'-acctgtttttgttccagtaccaggagccgatgaagaagatggtggg-3'
22. N509S, I514L	5'-catccaaaactaggagaaaattgctttcattctggttgggagtga-3' 5'-ggataaaattgctttcactctggttgggagtgatcacca-3' 5'-tggtgatcactcccaaccagagtgaaagcaattttatcc-3' 5'-tcactcccaaccagaatgaaagcaattttctcctagttttggatg-3'
23. N521S, E523T	5'-acctctgctcggcccagctccgtaaagctcttggcatccaaaactagg-3' 5'-cctagttttggatgccaagagctttacggagctgggccgagcagaggt-3'
24. I543V	5'-ctcgagctagatgggtacgaaggtaccatggaacc-3' 5'-ggttccatggtaccttcgtacccatctagctcgag-3'
25. Mouse BCO2+GKAA	5'-atgtcaaggtttgagccacctggtaaagctgcaactatgactgacaacac-3' 5'-gtgttgtcagtcatagttgcagctttaccaggtggctcaaaccttgacat-3'
26. Human BCO2-GKAA+A>T	5'-gtccaggtttgagctgcctatgactgacaatactaatg-3' 5'-cattagtattgtcagtcataggcagctcaaacctggac-3' 5'-tccaggtttgagctgcctaccatgactgacaata-3' 5'-tattgtcagtcatggtaggcagctcaaacctgga-3'
27. N-terminal switch	5’-atgaataaggtggacattgagatgc-3’ 5’-ccccgggctctttctttttg-3’ 5’-ttcgaaggaattcggtaccatgggaaatactcctcagaaaaaagc-3’ 5’-agcatctcaatgtccaccttattcataaagttggtctcagtgcag-3’ 5’-aaaacctgtattttcagggcgaaggagttcgaaccatgttgggaccgaagcaaag-3’ 5’-tctgttttttccagagtttcaatgtccactttattcataaaattagtctctgtgctc-3’

28. Human BCO2-GKAA with N122S	5'-tctcccggatccatgcaagagtatttttgaacgtttcatgtcc-3' 5'-ggacatgaaacgttcaaaaatactcttgcatggatccgggaga-3'
29. Human BCO2-GKAA with L133P	5'-atgtccaggtttgagccgcctaccatgactgac-3' 5'-gtcagtcatggtaggcggctcaaacctggacat-3'
30. Human BCO2-GKAA with Y435N, D437G	5'-ggcattgaatttcctcagatcaactatggtcgattcagtggcaaaaagta-3' 5'-tacttttgccactgaatcgaccatagttgatctgaggaaattcaatgcc-3'
31. Human BCO2-GKAA with S440N	5'-ttcctcagatcaactatggtcgattcaatggcaaaaagtatc-3' 5'-gatacttttgccattgaatcgaccatagttgatctgaggaa-3'
32. Human BCO2-GKAA with L133P and S440N	5'-atgtccaggtttgagccgcctaccatgactgac-3' 5'-gtcagtcatggtaggcggctcaaacctggacat-3' 5'-ttcctcagatcaactatggtcgattcaatggcaaaaagtatc-3' 5'-gatacttttgccattgaatcgaccatagttgatctgaggaa-3'

Fig. S1

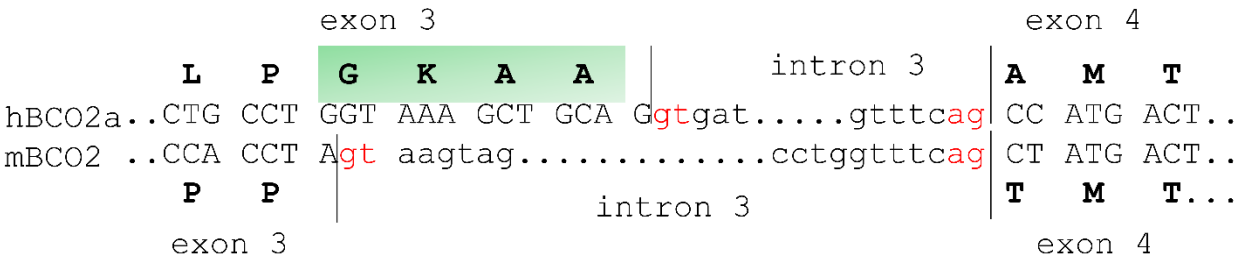
exon 3
exon 4
L P G K A A
intron 3
A M T
hBCO2a..CTG CCT GGT AAA GCT GCA Ggtgat.....gtttcag CC ATG ACT..
mBCO2 ..CCA CCT Agt aagtag.....cctggtttcag CT ATG ACT..
P P
intron 3
T M T...
exon 3
exon 4

Fig. S2

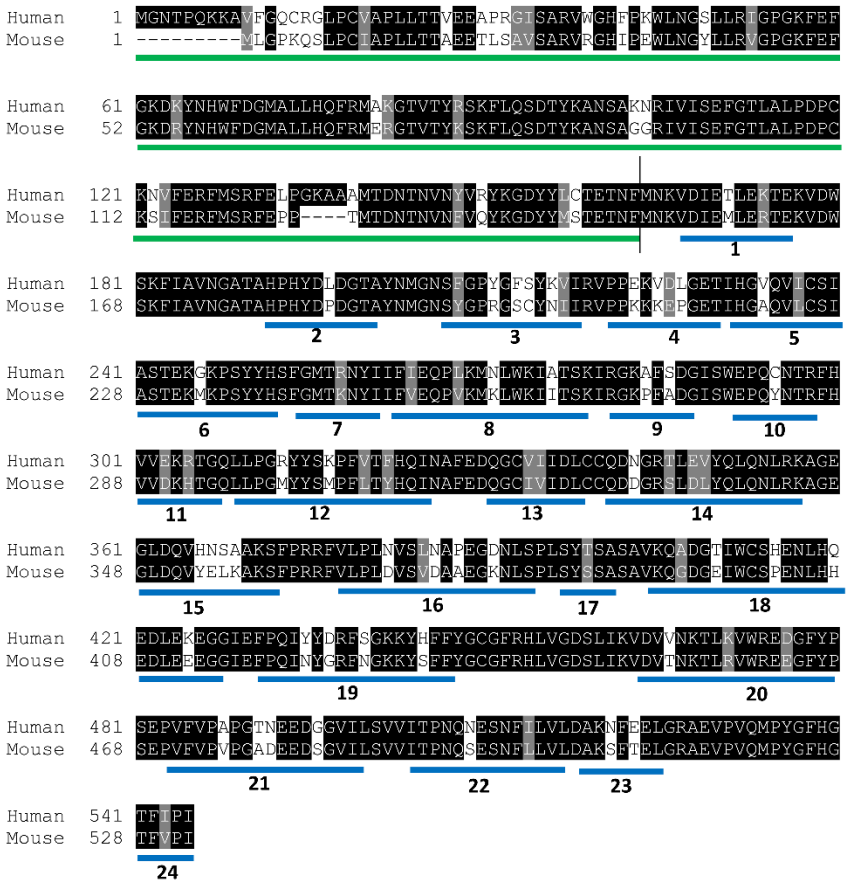
Human 1 MGNTPQKKAVFGQCRGLPCVAPLLTTVEEAPRGISARVWGHFPKWLNGSLLRIGPGKFEF
Mouse 1 ---------MLGPKQSLPCIAPLLTTAEETLSAVSARVRGHIPEWLNGYLLRVGPGKFEF
Human 61 GKDKYNHWFDGMALLHQFRMAKGTVTYPSKFLQSDTYKANSAKNRIVISEFGTLALPDPC
Mouse 52 GKDRYNHWFDGMALLHQFRMEEGTVTYKSKFLQSDTYKANSAGGRIVISEFGTLALPDPC
Human 121 KNVFERFMSRFELPGKAAAMTDNTNVNYVRYKGDYYLCTETNFMNKVDIETLEKTEKVDW
Mouse 112 KSIFERFMSRFEPP----TMTDNTNVNFVQYKGDYYMSTETNFMNKVDIEMLERTEKVDW
1
Human 181 SKFIAVNGATAHPHYDLDGTAYNMGNSFGPYGFSYKVIRVPPEKVDLGETIHGVQVLCSI
Mouse 168 SKFIAVNGATAHPHYDPDGTAYNMGNSYGPRGSCYNIIRVPPKKKPPGETIHGAQVLCSI
2 3 4 5
Human 241 ASTEKGKPSYYHSFGMTRNYIIFIEQPLKMNLWKIATSKIRGKAFSDGISWEPQCNTRFH
Mouse 228 ASTEKMKPSYYHSFGMTKNYIIFVEQPVKMKLWKIITSKIRGKPFADGISWEPQYNTRFH
6 7 8 9 10
Human 301 VVEKRTGQLLPGRYYSKPFVTFHQINAFEDQGCVIIDLCCQDNGRILEVYQLQNLRKAGE
Mouse 288 VVDKHTGQLLPGMYYSMPFLTYHQINAFEDQGCIVIDLCCQDDGRSLDLYQLQNLRKAGE
11 12 13 14
Human 361 GLDQVHNSAAKSFPRRFVLPLNVSLNAPEGDNLSPLSYTSASAVKQADGTIWCSHENLHQ
Mouse 348 GLDQVYELKAKSFPRRFVLPLDVSVDAAEGKNLSPLSYSSASAVKQCDGEIWCSPENLHH
15 16 17 18
Human 421 EDLEKEGGIEFPQIYYDRFSGKKYHFFYGCGFRHLVGDSLIKVDVVNKTLKVWREDGFYP
Mouse 408 EDLEEEGGIEFPQINYGRFNGKKYSFFYGCGFRHLVGDSLIKVDVTNKTLRVWREEGFYP
19 20
Human 481 SEPVFVPAPGTNEEDGGVILSVVITPNQNESNFILVLDAKNFEELGRAEVPVQMPYGFHG
Mouse 468 SEPVFVPVPGADEEDSGVILSVVITPNQSESNFLLVLDAKSFTELGRAEVPVQMPYGFHG
21 22 23
Human 541 TFIPI
Mouse 528 TFVPI
24

Fig. S3

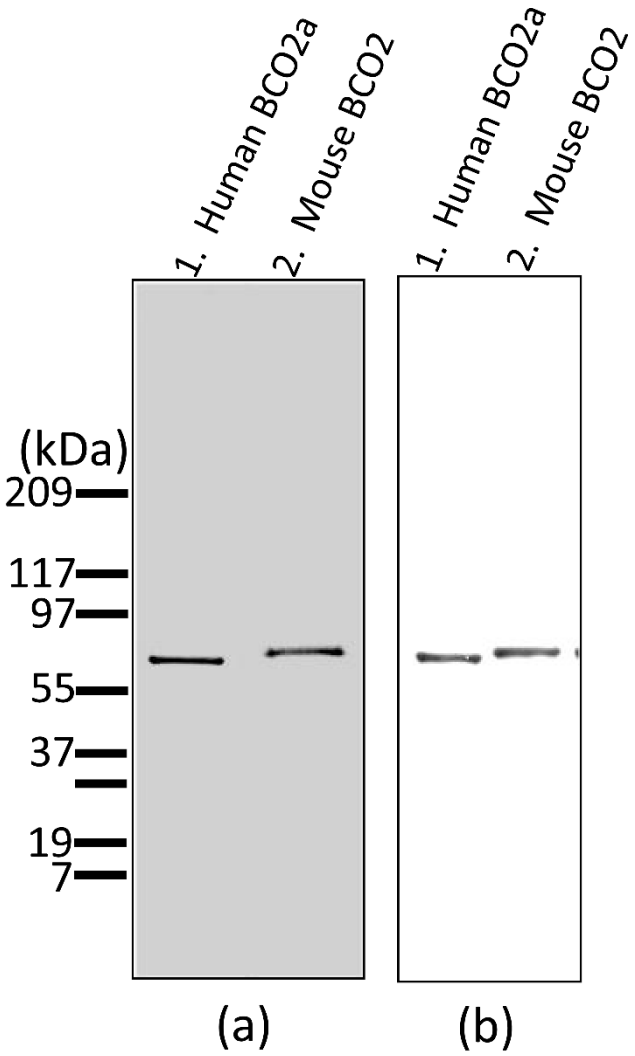
1. Human BCO2a
2. Mouse BCO2
1. Human BCO2a
2. Mouse BCO2
(kDa)
209
117
97
55
37
19
7
(a)
(b)

Fig. S4

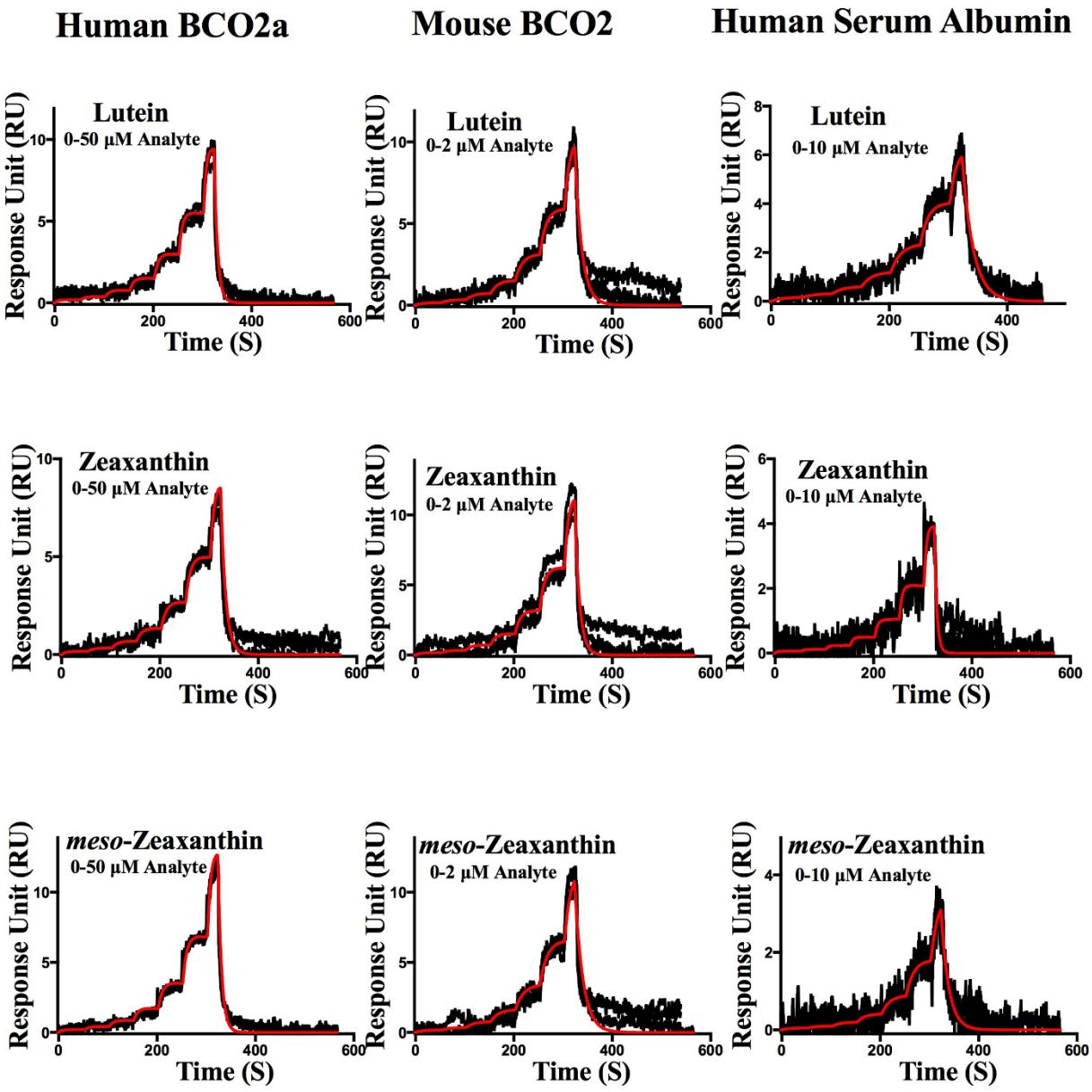
Human BCO2a
Mouse BCO2
Human Serum Albumin
Lutein
0-50 µM Analyte
Lutein
0-2 µM Analyte
Lutein
0-10 µM Analyte
Zeaxanthin
0-50 µM Analyte
Zeaxanthin
0-2 µM Analyte
Zeaxanthin
0-10 µM Analyte
meso-Zeaxanthin
0-50 µM Analyte
meso-Zeaxanthin
0-2 µM Analyte
meso-Zeaxanthin
0-10 µM Analyte
Response Unit (RU)
Time (S)